PHYSICSAccess Research Paper
ISSN Online: 2756-3898, ISSN Print: 2714-500X https://doi.org/10.47514/phyaccess.2026.6.2.016

Digital Holographic Interferometry for Ethylene Glycol Quality Control

David E Onsombi[1], Geoffrey Rurimo[2], Jack Kihiko[1], and Stephen M Njoroge[1]

[1] Department of Biological and Physical Sciences, Karatina University, Karatina, Kenya
[2] National Institute of Optics and Lasers, Multimedia University of Kenya, Nairobi, Kenya

Corresponding E-mail: snjoroge@karu.ac.ke

Received 13-07-2026
Accepted for publication 01-09-2026
Published 15-09-2026

Abstract

Digital holographic interferometry is a non-contact, full-field optical technique for quantifying sample-induced phase variations in transparent liquids. It offers a non-destructive approach for assessing composition-related changes in ethylene glycol. In this study, a Mach–Zehnder off-axis digital holographic interferometry system was constructed using a 632.8 nm helium–neon laser as the coherent illumination source. The laser output was assessed for power stability, after which the beam was spatially filtered and used to record holograms of pure ethylene glycol and ethylene glycol–water mixtures containing 0.1–80% v/v water. The holograms were reconstructed using Fourier-domain sideband filtering. Using the stabilized reconstructed dataset and literature refractive-index data as an external phase-order constraint, the literature-constrained optical path-difference estimate increased from 1.269 μm at 0.1% v/v water to 778.811 μm at 80% v/v water, demonstrating a concentration-dependent optical response. The developed system provides a proof-of-concept basis for literature-constrained, full-field ethylene glycol composition monitoring.

Keywords: Digital holographic interferometry; Mach–Zehnder interferometer; ethylene glycol; water adulteration; optical path difference; refractive index; phase reconstruction; Fourier filtering.

I. Introduction

Ethylene glycol (EG) is an important industrial liquid that is used in the manufacture of coolants, polyester, and various solvents, including automotive antifreeze. Its utility depends greatly on its purity and the stability of its optical and thermophysical properties. Water contamination is important because the refractive index of water is lower than that of pure EG; therefore, an increase in the water fraction changes the optical path of a laser beam travelling through the mixture. The proposal motivating this work identified the need for a rapid, non-destructive technique capable of monitoring EG quality through phase and refractive-index changes rather than relying solely on conventional offline methods.

Although traditional methods for purity assessment, such as gas chromatography and refractometry, are well established, they do not fully provide the spatially resolved, real-time, non-contact monitoring required for transparent liquids. Chromatographic methods are accurate, although they require sample handling and can be time-consuming for in-line screening [1–2]. Spectroscopic techniques are fast (e.g., UV–Vis, FTIR, and NIR), but they typically yield an integrated spectral signature rather than a full-field optical phase map [3–4]. Some recent fiber-optic refractive-index sensors have also been shown to be sensitive to EG–water mixtures; however, these sensors typically measure changes in the evanescent field and do not usually provide a two-dimensional phase distribution [5].

Digital holographic interferometry (DHI) is a coherent optical measurement method in which the interference pattern formed by reference and object waves is recorded digitally and

reconstructed numerically. DHI has been applied to quantitative phase imaging, refractive-index mapping, liquid-concentration measurements, and fluid diagnostics [6–12]. The reconstructed phase is proportional to the sample-induced optical path change, while the full-field measurement provides a two-dimensional phase distribution rather than a single spatially averaged value.

The contribution of the present study is application-specific rather than the introduction of DHI itself. The work applies full-field, single-wavelength, off-axis DHI to a controlled ethylene glycol–water concentration series and explicitly separates spatial phase unwrapping from the remaining global integer phase-cycle ambiguity. Published refractive-index information was only used to constrain the physically plausible wavelength order, and the resulting optical quantities are reported as literature-constrained estimates. This transparent treatment of the single-wavelength ambiguity, together with the intended ethylene glycol quality-monitoring application, constitutes the principal novelty of the study [7], [14–15].

This study is aimed at developing and evaluating a Mach–Zehnder off-axis DHI system for detecting water-induced optical changes in EG–water mixtures. The study comprised optical alignment and beam preparation, validation of hologram acquisition and Fourier reconstruction, extraction of residual OPD values relative to a pure-EG reference, and development of a reproducible, literature-constrained procedure for treating the integer phase-cycle ambiguity inherent in the single-wavelength configuration.

II. Materials and Methods

A. Holographic Recording Setup

A Mach–Zehnder off-axis digital holographic interferometry system was developed, and the laser output power was measured along the experimental optical path using a power meter. Spectral stability was assessed using a Fabry–Perot spectrum analyzer and a cathode-ray oscilloscope by observing the transmission peaks after aligning the laser beam with the Fabry–Perot cavity [16–18].

The laser beam was spatially filtered using a 10× microscope objective, a 15-µm pinhole, an iris diaphragm, and a collimating lens before entering the interferometer. A 50:50 beam splitter divided the filtered beam into object and reference arms. The object arm passed through a cuvette containing the ethylene glycol–water sample, while the reference arm bypassed the cuvette. The two beams were recombined at a second beam splitter and directed to a Thorlabs Zelux Series 1.6 MP monochrome CMOS camera (CS165MU/CS165MU1), positioned approximately 12 cm from the recombining beam splitter. The camera had a resolution of 1440 × 1080 pixels, a square pixel pitch of 3.45 µm, 10-bit monochrome digitization stored in a 16-bit TIFF container, and an exposure time of 0.410 ms. One mirror was adjusted to introduce an off-axis angle of approximately 2.23° between the object and reference beams at the camera plane. The liquid path length was 10.00 ± 0.01 mm.

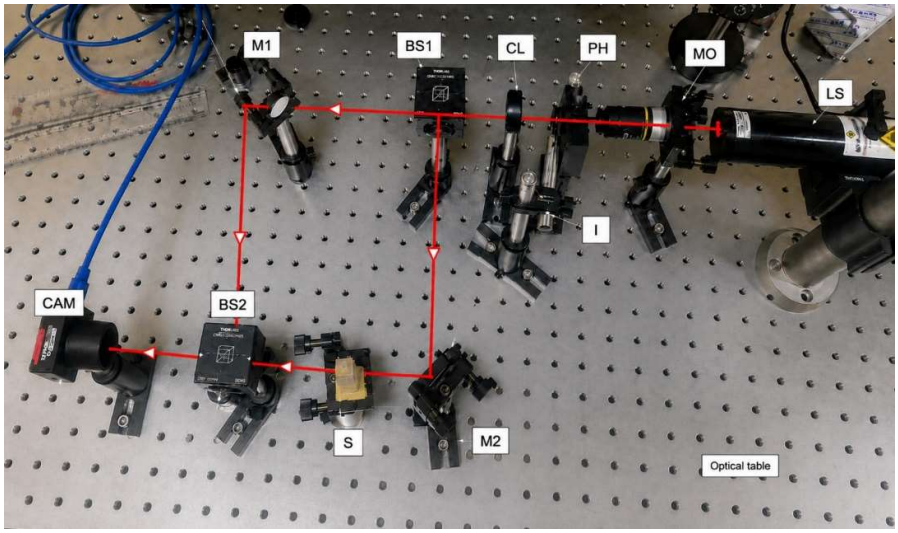

Fig. 1. Mach–Zehnder off-axis Digital Holographic Interferometry (DHI) setup. LS – He–Ne laser source; MO – 10× microscope objective; PH – 15 µm pinhole; I – iris diaphragm; CL – collimating lens; BS1 – first 50:50 beam splitter; BS2 – second 50:50 beam splitter; M1–M2 – mirrors; S – sample (10 mm optical cuvette); CAM – Thorlabs Zelux monochrome CMOS camera.

B. Digital Reconstruction

Each recorded 30-frame TIFF stack was averaged before reconstruction to reduce frame-to-frame intensity variation. The averaged holograms were reconstructed in MATLAB using an off-axis Fourier reconstruction algorithm. A two-dimensional fast Fourier transform was applied to each

averaged hologram, and the same fixed circular Fourier filter was used for all samples to isolate the positive first-order sideband. The isolated sideband was shifted to the centre of the Fourier spectrum and inverse Fourier transformed to obtain the complex optical field. The recorded hologram intensity was expressed using (1).

$$I(x,y) = |U_s(x,y) + U_r(x,y)|^2 \quad (1)$$

In (1), $U_s(x,y)$ is the sample-modified object field, and $U_r(x,y)$ is the reference field [8], [19–20].

The reconstructed complex optical field was represented by (2).

$$U(x,y) = A(x,y)\, exp[i\varphi(x,y)] \quad (2)$$

where $A(x,y)$ is the reconstructed amplitude and $\varphi(x,y)$is the phase. The sample-induced phase difference relative to the pure-EG reference was obtained using the complex-ratio method in (3).

$$\Delta\varphi_{w(x,y)} = \arg[U_s(x,y)U_r*(x,y)] \quad (3)$$

The reconstructed phase map obtained from (3) was initially wrapped within the interval −π to +π. Spatial phase unwrapping was applied to remove local 2π discontinuities within each reconstructed map. Phase unwrapping, sideband filtering, and reference stability are important factors in quantitative phase reconstruction [21–23].

For consistency, the same central region of interest (ROI) was used for all holograms. The ROI covered the central 60% of the 1440 × 1080-pixel image, corresponding to $x = 288$–1152 pixels and $y = 216$–864 pixels. A first-order plane, $P(x,y) = ax + by + c$ was fitted to each spatially unwrapped phase-difference map. Only the linear tilt components $ax + by$ were removed, while the constant term and mean sample-induced phase offset were preserved. The same ROI, pure-EG reference-comparison method, and detrending procedure were therefore applied to all reported raw OPD values.

The optical path difference (OPD) was calculated from the unwrapped differential phase according to (4).

$$OPD_{\mathrm{raw}}(x,y) = \frac{\lambda}{2\pi}\Delta\varphi_u(x,y) \quad (4)$$

where $OPD_{\mathrm{raw}}(x,y)$ is the raw residual optical path difference at the image coordinates (x,y), λ is the illumination wavelength, and $\Delta\varphi_u(x,y)$ is the spatially unwrapped phase difference between the sample and the pure-EG reference. The factor 2π represents one complete phase cycle.

The corresponding refractive index change relative to the pure ethylene glycol reference was calculated as,

$$\Delta n = \frac{OPD}{L} \quad (5)$$

where Δn is the refractive index change relative to pure ethylene glycol, OPD is the corresponding optical path difference, and L is the internal optical path length of the liquid sample. In the present study, the illumination wavelength λ, and liquid path length L were $0.6328\,\mu$m, and 10.00 mm respectively.

For the raw reconstructed measurements, OPD in (5) corresponds to OPD_{raw} obtained from (4). The coordinates x and y denote the horizontal and vertical pixel coordinates, respectively, in the reconstructed phase map.

The pure-EG hologram was used as the reference. The signed refractive index difference was defined using (6). Because water has a lower refractive index than pure ethylene glycol, Δn_s is negative for the investigated mixtures. For concentration-response presentation, positive magnitudes were reported using (7); thus, an increasing $|\Delta n|$ represents a progressively larger decrease in refractive index relative to pure EG, rather than an increase in the physical refractive index.

$$\Delta n_s = n_{mix} - n_{EG} < 0 \quad (6)$$

$$|\Delta n| = |OPD| / L = |n_{mix} - n_{EG}| \quad (7)$$

Spatial phase unwrapping removes local 2π jumps across an image, but it does not determine the global number of complete phase cycles between independently recorded sample and reference states. In a single-wavelength system, the absolute OPD may therefore remain ambiguous by an integer multiple of the wavelength. Multiwavelength holography can resolve this ambiguity experimentally, whereas the present study used an external refractive-index constraint [7], [14–15].

Reference refractive indices were calculated for 632.8 nm and 30 °C. The refractive index of water $n_w = 1.331055$ was calculated using the IAPWS formulation [24]. The refractive index of pure ethylene glycol $n_{EG} = 1.427748$ was calculated using the corrected Sellmeier and thermal-coefficient parameters [25–26]. For the nominal preparation volume fraction φ_w, missing mixture values were interpolated using the Lorentz–Lorenz relation in (8), which has been successfully applied to EG–water systems [27]. The calculation was performed at the nominal measurement temperature of 30 °C.

$$\frac{({n_{mix}}^2-1)}{({n_{mix}}^2+2)} = \frac{\varphi_w({n_w}^2-1)}{({n_w}^2+2)} + \frac{(1-\varphi_w)({n_{EG}}^2-1)}{({n_{EG}}^2+2)} \quad (8)$$

For each concentration i, the literature-based reference OPD magnitude was calculated from the model-interpolated mixture index using (9). The published values were used only to identify the plausible wavelength interval and were not treated as independent confirmation of the DHI result.

$$D_{ref,i} = L|n_{mix,i}^{ref} - n_{EG}^{ref}| \quad (9)$$

For each non-negative integer m, a candidate total OPD was generated from the residual OPD magnitude reported in the original reconstruction analysis using (10):

$$D_i(m) = D_{raw,i} + m\lambda, \quad m = 0, 1, 2, \ldots \quad (10)$$

The literature-constrained order was selected reproducibly using (11) as the integer that minimized the residual difference from $D_{\mathrm{ref},i}$:

$$k_i^{(0)} = round[\frac{(D_{(ref,i)} - D_{(raw,i)})}{\lambda}] \quad (11)$$

$$D_{LC,i} = D_{(raw,i)} + k_i^{(0)}\lambda \quad (12)$$

$$|\Delta n_{LC,i}| = \frac{D_{LC,i}}{L} \quad (13)$$

Here, i denotes the water-concentration level, m is a trial integer phase-cycle order, $D_i(m)$ is the candidate total OPD

for the ith concentration, $D_{\mathrm{raw},i}$ is the reconstructed residual OPD obtained directly from the single-wavelength phase map, $D_{\mathrm{ref},i}$ is the literature-based reference OPD calculated from the model refractive index, and λ is the laser wavelength. The term $k_i^{(0)}$ is the selected literature-constrained integer phase-cycle order that gives the smallest difference between the candidate OPD and the reference OPD. $D_{\mathrm{LC},i}$ is the resulting literature-constrained OPD estimate, L is the optical path length of the liquid sample, and $\left|\Delta n_{\mathrm{LC},i}\right|$ is the corresponding magnitude of the literature-constrained refractive-index change. The literature-constrained OPD estimate and the corresponding refractive-index-change magnitude were calculated using (12) and (13), respectively.

The superscript (0) identifies a literature-constrained order rather than an independently measured absolute fringe order. At $L = 10.00\,mm$, one wavelength corresponds to $\Delta n = \lambda/L = 6.328 \times 10^{-5}$. The ±1 °C temperature accuracy, ±0.01 mm path-length tolerance, published-index uncertainty, and mixture-model uncertainty can therefore permit adjacent integer orders. Independent refractometer measurements or multiwavelength DHI would be required to verify the absolute order experimentally. The resulting values are consequently described as literature-constrained OPD and refractive-index-change estimates.

C. Ethylene Glycol Quality Control

Pure ethylene glycol was used as the reference sample throughout the study. Distilled water was added volumetrically to prepare EG–water mixtures containing 0.1, 1, 5, 10, 20, 40, and 80% v/v water. Measurements were performed at a nominal temperature of $30 \pm 1^{\circ}C$ using a digital water bath. The stated uncertainty represents the water-bath accuracy and was considered when interpreting the temperature-dependent reference refractive indices. Each sample was transferred into the optical cuvette for hologram acquisition.

Table I. Volume Percentage Composition of Ethylene Glycol–Water Mixtures Used in the Experiment.

Ethylene Glycol (% vol)	100	99.9	99	95	90	80	60	20
Water (% vol)	0	0.1	1	5	10	20	40	80

For each concentration, four holograms were recorded under identical experimental conditions to minimize the effects of fringe-contrast variation, cuvette repositioning, beam-alignment fluctuations, and temporal instability. The digital reconstruction procedure described in Section B was used to reconstruct the recorded holograms. The reconstructed phase maps were then converted into optical path difference (OPD) and refractive-index change Δn using (4)–(6). These parameters were then used to assess the optical response of the EG–water samples to increasing water concentration.

III. Results and Discussion

A. Results

The laser output remained stable along the optical path used for the experiment, while repeated Fabry–Perot transmission peaks observed on the cathode-ray oscilloscope indicated stable spectral operation during the measurement period. Following spatial filtering and beam recombination, clear, straight off-axis interference fringes were recorded at the camera plane. The fringe pattern provided the spatial carrier required for isolation of the positive first-order sideband during Fourier-domain reconstruction. These observations indicated that the optical system produced holograms suitable for subsequent ethylene glycol–water measurements [9], [28].

Several pure-EG holograms were assessed to establish a stable phase baseline for EG–water reconstruction. The final reference hologram was selected from the pure-EG reference series based on frame-to-frame intensity stability, clear off-axis fringes, and a well-separated first-order Fourier sideband. This ensured that the EG–water sample holograms were compared against a stable pure-EG optical baseline.

For each water concentration, the recorded hologram stacks were reconstructed using the same fixed workflow: 30-frame averaging, Fourier-domain sideband filtering, complex-field reconstruction, wrapped-phase extraction, spatial phase unwrapping, first-order plane detrending, and conversion of the mean residual phase to OPD. The concentration series was processed as hologram sets under identical reconstruction conditions, with reports on the reconstructed raw phase, raw OPD, and refractive-index-change magnitude used for the concentration-response analysis presented in Table II.

Table II. Reconstructed hologram dataset used for the concentration-response analysis

Water (% v/v)	Hologram set	Raw phase (rad)	Raw OPD (μm)	|Δn|
0.1	11, 13, 14, 15	0.028920	0.002913	2.913e-07
1	16, 17, 18, 19	0.256083	0.025791	2.579e-06
5	20, 19, 18, 17	0.957762	0.096459	9.646e-06
10	21, 22, 23, 26	1.138373	0.114649	1.146e-05
20	31, 32, 34, 36	2.238250	0.225421	2.254e-05
40	38, 45, 44, 40	4.411210	0.444267	4.443e-05
80	51, 52, 53, 54	4.637119	0.467019	4.670e-05

The raw residual OPD values reported before the addition of any integer wavelength cycles in Table II represent the single-wavelength residual OPD obtained directly from the reconstructed phase maps. The OPD and refractive index quantities are reported as positive magnitudes. The corresponding refractive-index-change magnitudes were calculated using (7), where $L = 10{,}000$ µm. The signed physical refractive index change is expected to be negative because water has a lower refractive index than pure ethylene glycol.

Representative reconstruction panels for the 1% and 5% EG–water samples are presented in Figs. 2 and 3, respectively, to illustrate the processing sequence from the recorded hologram to the corresponding residual OPD map.

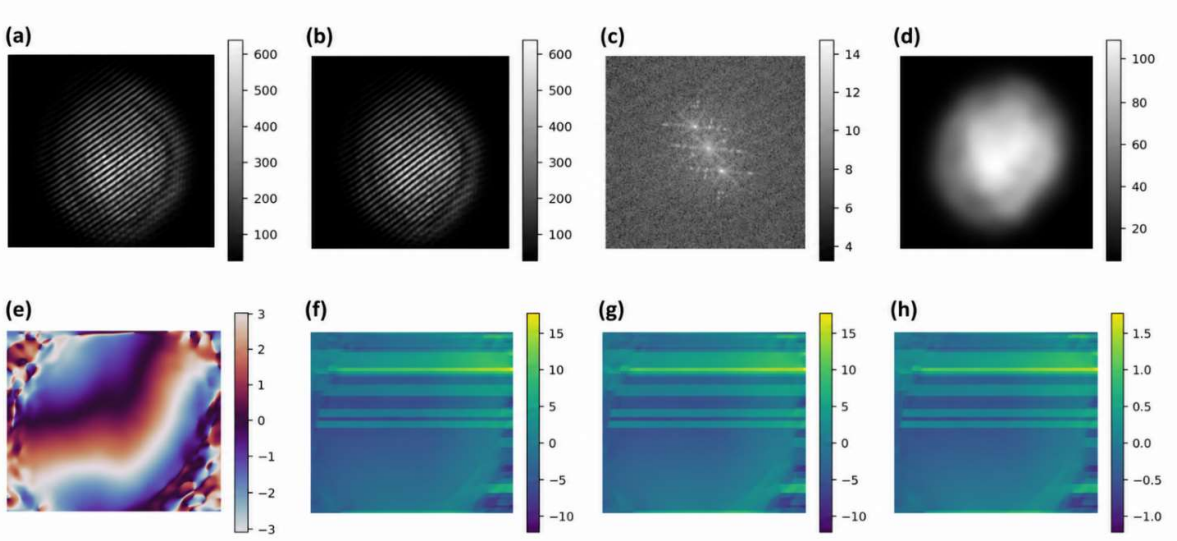

Fig. 2**.** Digital holographic reconstruction of the 1% water-in-ethylene-glycol sample relative to the pure-EG reference. The raw residual OPD magnitude was 0.025791 µm. (a) Reference hologram; (b) sample hologram; (c) Fourier spectrum; (d) reconstructed amplitude; (e) wrapped phase difference; (f) spatially unwrapped phase difference; (g) detrended phase map; and (h) OPD map.

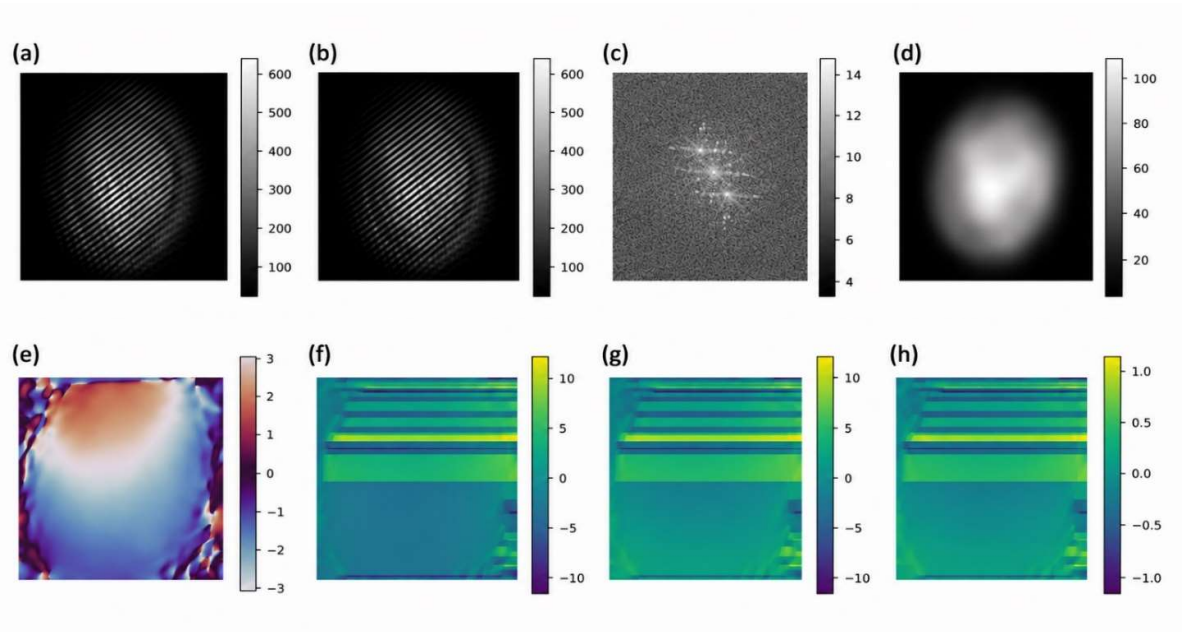

\

Fig. 3. Digital holographic reconstruction of the 5% water-in-ethylene-glycol sample relative to the pure-EG reference. The raw residual OPD magnitude was 0.096459 µm. (a) Reference hologram; (b) sample hologram; (c) Fourier spectrum; (d) reconstructed amplitude; (e) wrapped phase difference; (f) spatially unwrapped phase difference; (g) detrended phase map; and (h) OPD map.

The raw OPD magnitude increased from 0.002913 µm at 0.1% v/v water to 0.467019 µm at 80% v/v water in the dataset. These raw values represent residual single-wavelength OPD quantities obtained directly from the reconstructed phase maps. Although spatial phase unwrapping removes local 2π discontinuities within each phase map, it does not determine the remaining global integer-wavelength order between the independently recorded pure-EG reference and sample holograms. The raw OPD values are therefore reported separately from the literature-constrained OPD estimates in Table III. The variation of the raw residual OPD magnitude with water concentration is shown in Fig. 4.

Table III. Literature-constrained phase-cycle order calculation using the reconstructed dataset from Table II.

Water (% v/v)	Raw OPD D_{raw}	Model n_{mix}	Reference OPD D_{ref} (µm)	$k^{(0)}$	Literature-constrained OPD estimate $D_{LC,i}$ (µm)	$\lvert \Delta n_{LC,i} \rvert$
0.1	0.002913	1.427648	1.000224	2	1.268513	1.269e-04
1	0.025791	1.426748	9.999030	16	10.150591	1.015e-03
5	0.096459	1.422755	49.924038	79	50.087659	5.009e-03
10	0.114649	1.417780	99.671413	157	99.464249	9.946e-03
20	0.225421	1.407883	198.643536	314	198.924621	1.989e-02
40	0.444267	1.388293	394.547786	623	394.678667	3.947e-02
80	0.467019	1.349889	778.585201	1230	778.811019	7.788e-02

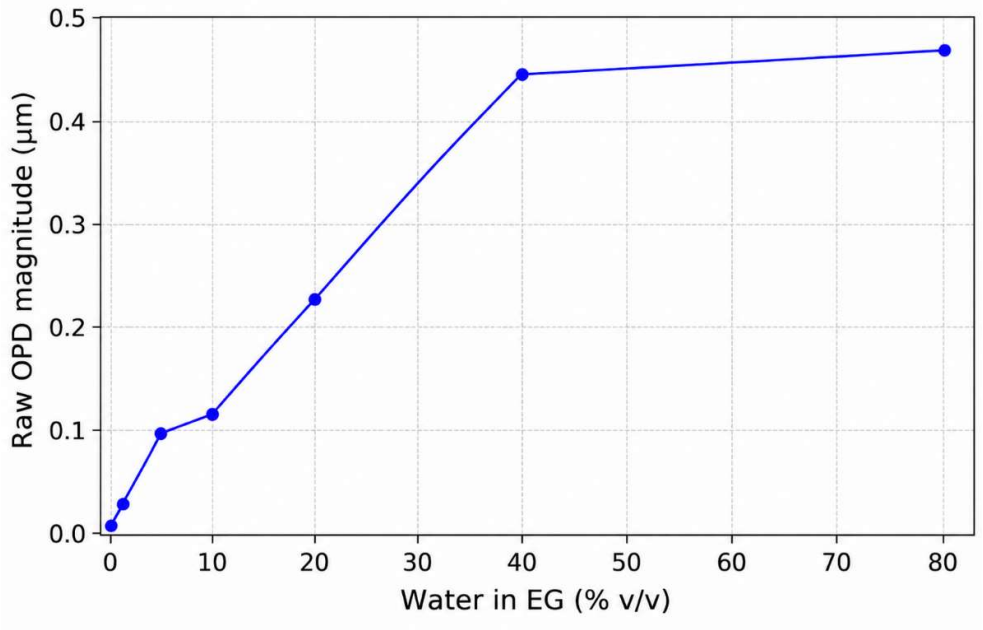

Fig. 4. Raw residual OPD magnitude as a function of water concentration in ethylene glycol. The plotted values represent single-wavelength residual OPD magnitudes obtained directly from the reconstructed phase maps before the addition of integer wavelength cycles.

The residual OPD values in Table II were used to calculate the integer phase-cycle order using the same external refractive-index procedure described in the reconstruction method. For each concentration i, the expected reference OPD magnitude, $D_{\mathrm{ref},i}$, was obtained from the model-interpolated EG–water refractive index using (9). Candidate OPD values were generated using (10), where $m = 0,1,2,\ldots$ and $\lambda = 0.6328$ µm. The integer order was then calculated reproducibly using (11). The literature-constrained OPD estimate was calculated using (12), and the corresponding magnitude of the refractive-index change was calculated using (13), with $L = 10{,}000$ µm.

This procedure uses literature refractive-index data only to identify the nearest physically plausible wavelength interval. The resulting $k_i^{(0)}$ values are therefore literature-constrained estimates rather than independently measured fringe orders. This approach avoids treating the assigned $k_i^{(0)}$ values as direct experimental observations and makes the role of the external refractive-index constraint explicit.

The $k_i^{(0)}$ values in Table III should therefore be interpreted as literature-constrained phase-cycle orders rather than independently measured fringe orders. The literature-constrained OPD estimates are useful for presenting the physically plausible concentration response; however, independent refractometer measurements or multiwavelength DHI would be required to validate the absolute order experimentally.

The resulting literature-constrained OPD magnitude and refractive-index-change magnitude as functions of water concentration are presented in Fig. 5.

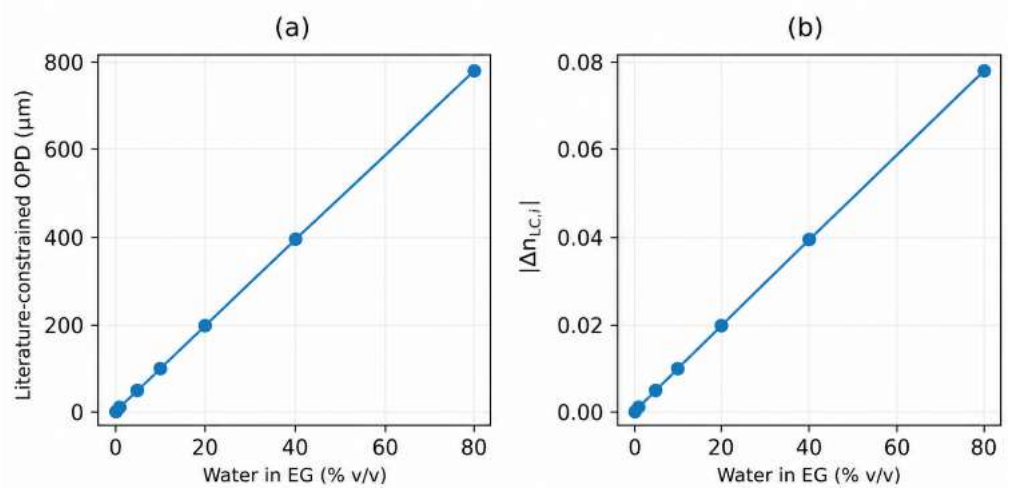

Fig. 5. Literature-constrained EG–water optical response calculated from the reconstructed dataset: (a) literature-constrained OPD magnitude and (b) magnitude of the literature-constrained refractive-index-change estimate relative to pure ethylene glycol. These values use the literature-constrained wavelength order $k_i^{(0)}$ and are not independent absolute refractive-index measurements.

B. Discussion

The results are interpreted by distinguishing the directly reconstructed residual OPD from the literature-constrained OPD estimate. The residual OPD values in Table II are the quantities obtained directly from the reconstructed single-wavelength phase maps after frame averaging, Fourier filtering, spatial unwrapping, plane detrending, and conversion of phase to OPD. They show the observable DHI response of the stabilized reconstructed dataset but do not represent complete absolute optical path differences because an unknown whole-wavelength component may remain in a single-wavelength measurement [8], [19–23].

The literature-constrained values in Table III should therefore be interpreted as model-constrained estimates rather than direct experimental OPD measurements. This distinction prevents the raw residual response and the literature-constrained response from being interpreted as the same result. The residual values demonstrate that the interferometer was sensitive to composition-related optical changes, while the literature-constrained values show the physically plausible order of magnitude when an external refractive-index constraint is applied.

The integer phase-cycle order k was calculated using the explicit rule in (11), where $D_{\mathrm{ref},i}$ was obtained from the external ethylene glycol–water refractive-index model and $D_{\mathrm{raw},i}$ was the reported residual OPD. This makes the role of the external refractive-index information explicit and reproducible.

It is important to distinguish this operation from ordinary spatial phase unwrapping. Spatial phase unwrapping removes local 2π discontinuities within a reconstructed phase map, whereas the $k\lambda$ term addresses the remaining global integer-wavelength ambiguity between independently recorded reference and sample states. A single-wavelength Mach–Zehnder DHI arrangement cannot determine this global order by itself; it requires either an external refractive-index constraint, multiwavelength DHI, or independent refractometer measurements [7], [14–18], [22].

Because the same literature model is used to select the wavelength interval, agreement between the literature-constrained DHI estimates and the model should not be presented as independent validation.

The hologram stacks were reconstructed using a uniform processing workflow to maintain consistency across the concentration series. The reconstruction procedure included 30-frame averaging, Fourier-domain sideband filtering, spatial phase unwrapping, first-order plane detrending, and conversion of phase to OPD. Before the final concentration-response values were reported, the reconstructed holograms were assessed for optical stability based on liquid settling, fringe visibility, temporal fluctuation, reference correlation, and first-order Fourier sideband separation. These checks helped ensure that the reported OPD values were obtained

from stable hologram records rather than from transient acquisition conditions [8–10], [19–23].

A preliminary sensitivity assessment was performed using stabilized pure-EG blank measurements and the low-concentration response between 0.1% and 1% water. From this analysis, the preliminary limit of detection was estimated as 0.0115% v/v water, while the preliminary limit of quantification was estimated as 0.0385% v/v water. These values indicate that the reconstructed DHI response is sensitive to small water-induced optical changes in ethylene glycol. However, they should be interpreted as preliminary method-development estimates, since more complete validation would require a larger blank-noise dataset, full replicate statistics across all concentrations, uncertainty propagation, and independent refractive-index validation.

The main sources of uncertainty in the present measurement include the cuvette path length, temperature stability, sample preparation, reference selection, residual carrier removal, Fourier-sideband filtering, and the refractive-index model used to determine the literature-constrained integer order k. For a 10.00 mm optical path length, one laser wavelength corresponds to $\lambda/L = 6.328 \times 10^{-5}$ in refractive-index units. Therefore, an error of one integer phase cycle would change the literature-constrained $|\Delta n|$ estimate by 6.328×10^{-5}. This effect is relatively small for the higher-concentration mixtures but becomes important at low water concentrations. In addition, the cuvette path length of 10.00 ± 0.01 mm contributes approximately 0.1% relative uncertainty, while the nominal 30 ± 1 °C measurement condition must be considered because the refractive indices of both water and ethylene glycol are temperature dependent [24–26].

The refractive-index changes reported in Tables II and III are presented as magnitudes. Since water has a lower refractive index than pure ethylene glycol, increasing the water fraction reduces the refractive index of the mixture. The signed refractive-index change is therefore negative, as defined in (6). In this study, $|\Delta n|$, as given in (7), is reported to show the magnitude of the optical change relative to pure EG. Thus, an increasing $|\Delta n|$ represents a progressively larger decrease in refractive index, not an increase in the actual refractive index of the mixture.

The literature refractive-index values used in this work provide an external constraint for estimating the integer phase-cycle order. The model n_{mix} values in Table III were obtained from published refractive-index data for water and ethylene glycol together with Lorentz–Lorenz mixture interpolation. This approach provides a physically reasonable basis for estimating the wavelength order and the corresponding literature-constrained OPD values. However, the comparison should be interpreted as a literature-based consistency check rather than as independent experimental validation. Direct validation would require refractive index measurements of the same prepared mixtures using an independently calibrated refractometer under comparable temperature and wavelength conditions.

The results therefore support a proof-of-concept application of off-axis DHI for detecting composition-related optical changes in ethylene glycol–water mixtures. The method is potentially useful because, unlike conventional refractometry, DHI can provide a spatial phase map across the sample field. This full-field capability may be valuable for identifying non-uniform mixing, local contamination, or temperature-related refractive-index gradients. Nevertheless, routine quality-control application would require further development, including a validated calibration curve, independent refractive-index comparison, repeatability statistics, uncertainty propagation, and experimentally confirmed detection thresholds [9–13], [28–29].

IV. Conclusion

A Mach–Zehnder off-axis digital holographic interferometry system was applied to ethylene glycol–water mixtures and produced measurable residual phase and OPD responses following Fourier-domain reconstruction. The directly reconstructed OPD values were treated as residual single-wavelength quantities, while literature-constrained OPD estimates were used to account for the remaining integer phase-cycle ambiguity.

The results showed a concentration-dependent optical response with increasing water concentration. The integer phase-cycle orders were calculated using published refractive-index data rather than being treated as directly measured fringe orders; therefore, the literature-constrained values remain physically plausible estimates that require independent validation.

A preliminary limit of detection of 0.0115% v/v water and a preliminary limit of quantification of 0.0385% v/v water were estimated from stabilized pure-EG blank measurements and the low-concentration response. Overall, the study demonstrates DHI as a proof-of-concept technique for ethylene glycol composition monitoring, with future work required to address replicate statistics, uncertainty analysis, refractometer validation, and multiwavelength phase-order confirmation.

Acknowledgement

I acknowledge the guidance of my supervisors, the support of Karatina University, and the NIOL laboratory facilities used during optical alignment and hologram acquisition.

Data Availability

The processed hologram metrics, reconstruction graphs, and manuscript figures are available from the author. Raw multi-frame TIFF hologram stacks are available upon reasonable request due to their file size.

Conflict of Interest

The author declares no competing interests.

References

[1] C. Fan, Y. Zhang, C. Wang, Z. Peng, and Z. Gao, "Determination of purity and impurities of ethylene glycol for industrial use by gas chromatography," *Se Pu*, vol. 37, no. 1, pp. 116–120, 2019, doi: 10.3724/SP.J.1123.2018.08030.

[2] Agency for Toxic Substances and Disease Registry, *Toxicological Profile for Ethylene Glycol*. Atlanta, GA, USA: U.S. Department of Health and Human Services, Public Health Service, Nov. 2010.

[3] F. Gaxiola, J. J. Leal, A. Manzo-Martínez, I. Salmerón, J. R. Linares-Morales, and R. Narro-García, "Identification of the beverage Sotol adulterated with ethylene glycol using UV-Vis spectroscopy and artificial neural networks," *Chemosensors*, vol. 12, no. 3, Art. no. 46, 2024, doi: 10.3390/chemosensors12030046.

[4] S. M. Obeidat and A. Y. Hammoudeh, "Simultaneous determination of glycerine and DEG in glycerine raw material using FT-IR spectroscopy and multivariate calibration methods," *International Journal of Applied Pharmaceutics*, vol. 17, no. 2, pp. 293–298, 2025, doi: 10.22159/ijap.2025v17i2.52729.

[5] R. M. A. Ayaz, A. Mustafa, and R. Funari, "Symmetrically etched plastic optical fiber sensor for the detection of ethylene glycol contamination in water," *Optical and Quantum Electronics*, vol. 57, Art. no. 626, 2025, doi: 10.1007/s11082-025-08556-8.

[6] C. Guerrero-Méndez, T. Saucedo-Anaya, M. Araiza-Esquivel, R. E. Balderas-Navarro, A. López-Martínez, and C. Olvera-Olvera, "Measurements of concentration differences between liquid mixtures using digital holographic interferometry," *Metrology and Measurement Systems*, vol. 24, no. 1, pp. 19–26, 2017, doi: 10.1515/mms-2017-0002.

[7] M. K. Kim, "Principles and techniques of digital holographic microscopy," *SPIE Reviews*, vol. 1, no. 1, Art. no. 018005, 2010, doi: 10.1117/6.0000006.

[8] V. Petrov, A. Pogoda, V. Sementin, A. Sevryugin, E. Shalymov, D. Venediktov, and V. Venediktov, "Advances in digital holographic interferometry," *Journal of Imaging*, vol. 8, no. 7, Art. no. 196, 2022, doi: 10.3390/jimaging8070196.

[9] G. Cubreli, P. Psota, P. Dančová, V. Lédl, and T. Vít, "Digital holographic interferometry for the measurement of symmetrical temperature fields in liquids," *Photonics*, vol. 8, no. 6, Art. no. 200, 2021, doi: 10.3390/photonics8060200.

[10] J.-M. Desse and F. Olchewsky, "Dual-reference digital holographic interferometry for analyzing high-density gradients in fluid mechanics," *Optics Letters*, vol. 43, no. 8, pp. 1635–1638, 2018, doi: 10.1364/OL.43.001635.

[11] J.-M. Desse, P. Picart, and P. Tankam, "Digital color holography applied to fluid and structural mechanics," *Optics and Lasers in Engineering*, vol. 50, no. 1, pp. 18–28, 2012, doi: 10.1016/j.optlaseng.2011.06.018.

[12] D. Ruiz-Cadalso and C. Furlong, "High-resolution imaging for in-situ non-destructive testing by quantitative lensless digital holography," *Frontiers in Photonics*, vol. 5, Art. no. 1351744, 2024, doi: 10.3389/fphot.2024.1351744.

[13] H. H. Wahba and T. Kreis, "Characterization of optical fibers by digital holographic interferometry," *Proc. SPIE*, vol. 7389, Art. no. 73890K, 2009, doi: 10.1117/12.826854.

[14] J. Gass, A. Dakoff, and M. K. Kim, "Phase imaging without 2π ambiguity by multiwavelength digital holography," *Optics Letters*, vol. 28, no. 13, pp. 1141–1143, 2003, doi: 10.1364/OL.28.001141.

[15] Y. Lee, Y. Ito, T. Tahara, J. Inoue, P. Xia, Y. Awatsuji, K. Nishio, S. Ura, and O. Matoba, "Single-shot dual-wavelength phase unwrapping in parallel phase-shifting digital holography," *Optics Letters*, vol. 39, no. 8, pp. 2374–2377, 2014, doi: 10.1364/OL.39.002374.

[16] T. Kreis, *Handbook of Holographic Interferometry: Optical and Digital Methods. Weinheim, Germany: Wiley-VCH, 2005*.

[17] P. Picart and J.-C. Li, Eds., Digital Holography. London, U.K.: ISTE Ltd.; Hoboken, NJ, USA: Wiley, 2012.

[18] U. Schnars and W. Jüptner, *Digital Holography: Digital Hologram Recording, Numerical Reconstruction, and Related Techniques*. Berlin, Germany: Springer, 2005.

[19] E. Cuche, P. Marquet, and C. Depeursinge, "Spatial filtering for zero-order and twin-image elimination in digital off-axis holography," *Applied Optics*, vol. 39, no. 23, pp. 4070–4075, 2000, doi: 10.1364/AO.39.004070.

[20] J. Zhang, S. Dai, C. Ma, T. Xi, J. Di, and J. Zhao, "A review of common-path off-axis digital holography: Towards high stable optical instrument manufacturing," *Light: Advanced Manufacturing*, vol. 2, no. 3, Art. no. 23, 2021, doi: 10.37188/lam.2021.023.

[21] Y. Chen, Q. Wang, G. Zhang, P. Li, Y. Fan, Z. Wang, and M. Dong, "Phase unwrapping in digital holography based on SRDU-Net," *Optics Communications*, vol. 573, Art. no. 131055, 2024, doi: 10.1016/j.optcom.2024.131055.

[22] C. Guerrero-Mendez, T. Saucedo-Anaya, I. Moreno, M. Araiza-Esquivel, C. Olvera-Olvera, and D. Lopez-Betancur, "Digital holographic interferometry without phase unwrapping by a convolutional neural network for concentration measurements in liquid samples," *Applied Sciences*, vol. 10, no. 14, Art. no. 4974, 2020, doi: 10.3390/app10144974.

[23] Y. Liu, Q. Sun, H. Chen, and Z. Jiang, "Fractional Fourier-transform filtering and reconstruction in off-axis digital holographic imaging," *Optics Express*, vol. 31, no. 6, pp. 10709–10719, 2023, doi: 10.1364/OE.483528.

[24] A. H. Harvey, J. S. Gallagher, and J. M. H. Levelt Sengers, "Revised formulation for the refractive index of water and steam as a function of wavelength, temperature, and density," *Journal of Physical and Chemical Reference Data*, vol. 27, no. 4, pp. 761–774, 1998, doi: 10.1063/1.556029.

[25] D. Jakubczyk, G. Derkachov, K. Nyandey, S. Alikhanzadeh-Arani, and A. Derkachova, "Chromatic dispersion and thermal coefficients of hygroscopic liquids: 5 glycols and glycerol," *Scientific Data*, vol. 10, Art. no. 894, 2023, doi: 10.1038/s41597-023-02819-3.

[26] D. Jakubczyk, G. Derkachov, K. Nyandey, S. Alikhanzadeh-Arani, and A. Derkachova, "Author correction: Chromatic dispersion and thermal coefficients of hygroscopic liquids: 5 glycols and glycerol," *Scientific Data*, vol. 11, Art. no. 727, 2024, doi: 10.1038/s41597-024-03547-y.

[27] O. Iulian, A. Stefaniu, O. Ciocirlan, and O. Croitoru, "Property prediction for binary and ternary systems with water, 1,4-dioxane and ethylene glycol. II. Refractive index," Revue Roumaine de Chimie, vol. 55, no. 8, pp. 475–480, 2010.

[28] C. Alvarez, B. Baskar, C. Berrospe-Rodriguez, S. Kavian, R. Sellers, M. J. Powell-Palm, and G. Aguilar-Mendoza, "Digital holography interferometry for refractive index characterization and temperature mapping of aqueous solutions at supercooled temperatures," *Laser & Photonics Reviews*, vol. 19, no. 9, Art. no. 2400921, 2025, doi: 10.1002/lpor.202400921.

[29] D. Khodadad, B. Tayebi, A. Saremi, and S. Paul, "Temperature sensing in space and transparent media: Advancements in off-axis digital holography and the temperature coefficient of refractive index," *Applied Sciences*, vol. 13, no. 14, Art. no. 8423, 2023, doi: 10.3390/app13148423.